Journal of Molecular Catalysis A: Chemical 297 (2009) 54–62

Contents lists available at ScienceDirect

Journal of Molecular Catalysis A: Chemical

journal homepage: www.elsevier.com/locate/molcata

# Effect of silver modification on structure and catalytic performance of Ni-Mg/diatomite catalysts for edible oil hydrogenation

Miroslav Stanković[a], Margarita Gabrovska[b,*], Jugoslav Krstić[a], Peter Tzvetkov[c], Maya Shopska[b], Tsenka Tsacheva[d], Predrag Banković[a], Rumeana Edreva-Kardjieva[b], Dušan Jovanović[a]

[a] Institute of Chemistry, Technology and Metallurgy, Department of Catalysis and Chemical, Engineering, Njegoševa 12, 11 000 Belgrade, Serbia
[b] Institute of Catalysis, Bulgarian Academy of Sciences, Acad. G. Bonchev str., bl. 11, 1113 Sofia, Bulgaria
[c] Institute of General and Inorganic Chemistry, Bulgarian Academy of Sciences, Acad. G. Bonchev str., bl. 11, 1113 Sofia, Bulgaria
[d] Institute of Physical Chemistry, Bulgarian Academy of Sciences, Acad. G. Bonchev str., bl. 11, 1113 Sofia, Bulgaria

ARTICLE INFO

*Article history:*
Received 26 May 2008
Received in revised form 1 September 2008
Accepted 5 September 2008
Available online 16 September 2008

*Keywords:*
Mg-Ni/diatomite catalyst
Silver modifier
Texture
Soybean oil hydrogenation activity
*cis–trans* isomerization

ABSTRACT

Silver modified Mg-Ni/diatomite materials with ratios of $SiO_2$/Ni = 1.07 and Mg/Ni = 0.1, differing in Ag content (Ag/Ni = 0.025 and 0.1) were prepared by the precipitation–deposition method. The effects of silver presence and content on the structure, morphology, texture and $H_2$-adsorption capacity of the obtained precursors were studied by X-ray diffraction, scanning electron microscopy, Hg-porosimetry and $H_2$-chemisorption techniques. The catalytic performance of the corresponding catalysts in the soybean oil hydrogenation was investigated. The increase of the silver loading resulted in the development of macroporosity and increase in the total sample porosity. The decrease of both $H_2$-adsorption capacity and hydrogenation activity are related to the metallic silver covering and blocking effects on the $Ni^{2+}$ species, thus hampering the access of hydrogen. The decrease of hydrogenation activity and favorable limiting of *cis–trans* isomerization on the silver modified catalyst are explained by Horiuti–Polanyi mechanism based on the assumption that hydrogenation and isomerization proceed at the same active metallic nickel sites *via* half-hydrogenated intermediates.

It was shown that the adjustment of the catalyst composition by changing the content of silver modifier offers the possibility to control the total amount of solid fat content, stearic acid and detrimental *trans* fatty acids in the hydrogenated derivatives. The catalyst with higher silver content is proposed as a promising candidate for selective edible oil hydrogenation catalyst.



## 1. Introduction

Vegetable oils represent complex mixtures of fatty acid esters in triglyceride form, usually of different degrees of un-saturation. The partial hydrogenation of the fats and oils continues to be one of the most universal ways to modify their physical properties, oxidative and thermal stability. The process is widely used in the elaboration of margarines, shortenings, bakery products, etc. [1].

The hydrogenation of vegetable oils using nickel slurry catalysts is a complex chemical process, which can be influenced by the control of operating variables such as temperature, hydrogen pressure, agitation and catalyst itself [2]. Batch processes in slurry reactors at high temperatures, low pressures, long reaction times and supported Ni catalysts are most commonly used in the oil industry. The carbon double bonds are partially or fully saturated during the hydrogenation. Concomitantly, the catalytic isomerization of naturally occurring *cis* fatty acids (CFAs) to *trans* fatty acids (TFAs) takes place [3]. The selectivity of the process represents a considerable challenge, aiming to enhance the hydrogenation rate of the double bonds saturation and simultaneously to suppress the isomerization [4].

Because of the negative health effects of *trans* fatty acids they have recently received increasing attention and are considered to be even more detrimental than the saturated ones [5]. Several alternatives have been studied to seek ways for substantial reduction of inevitable TFA content in the hydrogenated edible oils such as the electrocatalytic hydrogenation [6], supercritical fluid hydrogenation [7], membrane reactor technology [8], catalytic transfer hydrogenation [9], usage of monolithic catalysts [10] as well as

* Corresponding author. Tel.: +359 2 9793578; fax: +359 2 9712967.
*E-mail addresses:* mikastan@nanosys.ihtm.bg.ac.yu (M. Stanković), margo@ic.bas.bg (M. Gabrovska), jkrstic@nanosys.ihtm.bg.ac.yu (J. Krstić), p-tzvetkov@gmx.net (P. Tzvetkov), shopska@ic.bas.bg (M. Shopska), tsacheva@ipchp.ipc.bas.bg (T. Tsacheva), predragb@nanosys.ihtm.bg.ac.yu (P. Banković), rumedkar@ic.bas.bg (R. Edreva-Kardjieva), dusanmj@nanosys.ihtm.bg.ac.yu (D. Jovanović).

1381-1169/$ – see front matter © 2008 Elsevier B.V. All rights reserved.
doi:10.1016/j.molcata.2008.09.004

new catalyst development and modification [4,11,12] including supported precious metals [12–15].

The investigated catalysts offer different advantages but also have considerable shortcomings. However, the nickel catalysts commonly supported on modified natural earth, silica or alumina, are still used in the industry due to their good overall performance, i.e. high activity, high tailored linolenic and linoleic selectivity, low cost and easy removal from the processed oil by filtration [12]. The main disadvantage of nickel catalysts is the significant CFAs to TFAs isomerization [16–19]. Thus, the challenge for edible oil industry is the usage of novel modified Ni catalysts suppressing TFAs formation in the hydrogenated products.

Examining Ag-Ni supported catalysts for the selective fat hydrogenation, Lefèbvre and Baltes [11] reported the beneficial role of silver in the diminution of TFAs production. According to our knowledge, no other studies have been performed on a similar catalyst system for the edible oil hydrogenation by the present times.

In our earlier paper it has been published that Mg-Ni/diatomite catalyst manifests high activity in the hydrogenation of soybean oil. However, the amounts of formed TFAs were rather high [19]. In order to improve the catalyst performance, Mg-Ni/diatomite material was modified by the addition of silver.

This paper reports refined preliminary published results [20,21] and describes new data about the reduced Ag modified Mg-Ni/diatomite precursors. The properties of the modified precursors and catalysts are systematically compared to the non-modified ones. The effects of Ag modification on the texture, morphology, hydrogen adsorption capacity and catalytic performance of the materials will contribute to select the promising candidate for selective edible oil hydrogenation catalyst.

## 2. Experimental

### 2.1. Support

Diatomite (designation D), used as a supporting $SiO_2$ material was obtained from Baroševac – field B ("Kolubara" coal basin, Lazarevac, Serbia). Crude diatomite material was mechanically, chemically and thermally treated in order to obtain activated support. Detailed description of the equipment and the experimental conditions are given in ref. [18]. The composition of the activated diatomite is (wt%): $SiO_2$ – 93.07, $Al_2O_3$ – 3.87, MgO – 0.80, CaO – 0.59, $K_2O$ – 0.56, $Fe_2O_3$ – 0.56, and $Na_2O$ – 0.05.

### 2.2. Preparation of the precursors

The non-modified and silver modified precursors were obtained by the precipitation–deposition method using "*pro analyze*" purity grade nitrate salts of the corresponding metals and sodium carbonate as precipitant. The amounts of $SiO_2$, Ni and Mg in all precursor samples were the same ($SiO_2$/Ni = 1.07 and Mg/Ni = 0.1), while the amount of added Ag varied between the samples (Ag/Ni = 0.025 and 0.1).

Aqueous solutions of 0.33 M $Ni(NO_3)_2$, 0.033 M $Mg(NO_3)_2$, 0.033 M $AgNO_3$, 1.05 M $Na_2CO_3$ and aqueous suspension containing 2.0 wt% of diatomite were prepared. A fixed volume of mixed Mg–Ni nitrate or Ag–Mg–Ni nitrate solution was poured into a reaction vessel, equipped with a stirrer, thermometer and pH electrode. The solution was heated up to 60 °C and precipitated by drop wise addition of $Na_2CO_3$, controlled by a peristaltic pump, under vigorous stirring at constant value of pH 10.0 ± 0.1. The obtained precipitate was aged for 30 min at 60 °C followed by the increase of temperature up to 90 °C. The diatomite suspension was separately heated at 90 °C and added to the aged precipitate in a quantity sufficient to satisfy the molar ratio of $SiO_2$/Ni = 1.07. The resulting material was aged for another 30 min at 90 °C under constant stirring, filtered and thoroughly washed with hot distilled water (~90 °C). The samples were dried at 120 °C for 24 h and ground to a powder. The designation of the precursors corresponded to the Ag/Ni molar ratio, i.e. Ni-0 (silver free), AgNi-0.025 and AgNi-0.1.

### 2.3. Characterization of the support and precursors

The X-ray diffraction measurements were carried out on a Brucker D8 Advance powder diffractometer employing $CuK_\alpha$ radiation ($\lambda$ = 0.15418 nm), operated at $U$ = 40 kV and $I$ = 40 mA. Crystalline phases were identified using Joint Committee on Powder Diffraction Standards (JCPDS). The estimation of the mean metallic crystallite size was done using "A curve fitting and data analysis program fityk 0.8.6", based on the calculation of the integral breadth [22].

The scanning electron microscopy observations were carried out on a JEOL Superprobe 733 microscope with a 25 kV beam.

The mercury intrusion porosimetry was applied for the measurements of total intrusion volume, macro- and mesopore volume, pore size distribution (PSD) and total porosity. The porosimetric studies were performed on the automatic porosimeters Fisons – 2000 series (the limiting pressure of 200 MPa, pore diameter from 7.5 to 15000 nm) and Carlo Erba – 120 macropore unit (the limiting pressure of 0.1 MPa, pore diameter from 100,000 to 15,000 nm) supplied with data processing program Milestone 200.

The hydrogen-chemisorption measurements were carried out in a volumetric device. The samples were previously submitted to the reduction in the equipment at 430 °C for 5 h with a gas mixture of $H_2/N_2$ (1/1, v/v) at the heating rate of 2 °C $min^{-1}$. The adsorption isotherms were obtained at 25 °C and pressures in the range of 0–100 Torr (1 Torr = 133.3 Pa). More detailed description was presented in ref. [19].

### 2.4. Reduction of the precursors

The reduction (activation) of the precursors was performed in a laboratory set-up by a "dry reduction" method. The reduction process was accomplished with a gas mixture of $H_2/N_2$ (1/1, v/v) at the flow rate of 5 $dm^3$ $h^{-1}$. The reduction temperature was raised up to 430 °C at the heating rate of 1.5 °C $min^{-1}$ and held constant for 5 h. After cooling down to room temperature, the reduced precursors were impregnated with pure paraffin oil in order to diminish the exceptional pyrophority of the metallic nickel. A part of the reduced precursors were passivated with a mixture of 350 ppm of $O_2$ in nitrogen. The reduced-passivated precursors were denoted with the suffix red, i.e. Ni-$0_{red}$, AgNi-$0.025_{red}$ and AgNi-$0.1_{red}$.

### 2.5. Catalytic test

The partial soybean oil hydrogenation was performed in a 7.5 $dm^3$ three phase pilot plant batch slurry reactor under the following conditions: oil mass – 5000 g; catalyst concentration – 0.10 wt% with respect to the amount of oil; stirring rate – 750 rpm; initial hydrogenation temperature – 145 °C; final hydrogenation temperature – 160 °C; initial $H_2$ pressure – 0.08 MPa, and final $H_2$ pressure – 0.16 MPa.

The soybean oil hydrogenation activity of the studied catalysts is represented as the change of the starting oil iodine value (IV) with the reaction time in conformity with ISO 3961 [23] according to the expression:

$$\text{Conversion}\,(\%) = [\text{IV}_0 - \text{IV}_t)/\text{IV}_0] \times 100,$$

where $IV_0$ – initial iodine value at time $t = 0$ min and $IV_t$ – iodine value after $t = t$ min.

### 2.6. Analysis of the hydrogenated products

Refined soybean oil with constant fatty acid composition was used as the starting material. The oil fatty acid content was as follows (wt%): C14:0 – myristic 0.5, C16:0 – palmitic 11.1, C16:1 – palmitoleic 0.8, C18:0 – stearic 4.5, C18:1 – oleic 21.3, C18:2 – linoleic 53.8, C18:3 – linolenic 7.1, C20:0 – arachidic 0.3, C20:1 – eicosenoic 0.4, and C22:0 – behenic 0.2.

The change in the fatty acid composition of soybean oil during the hydrogenation was determined by taking probes at each 30 min.

The starting oil and the fractions of hydrogenated oil were converted into fatty acid methyl ester form by IUPAC method II.D.19 [24]. The concentration of fatty acid methyl esters was determined by capillary column gas chromatography [25]. An Agilent HP-88 (100 m × 0.25 mm I.D., 0.20 μm film thickness) capillary column was used for the analysis. The amount of $2 \times 10^{-6}$ $dm^{-3}$ of the probe was injected into a Shimadzu GC-9A gas chromatograph equipped with a splitter and flame ionization detector. Both the detector and the injector were maintained at 240 °C, whereas the column temperature was 180 °C. Helium was used as a carrier gas with the flow rate of 1.2 $cm^3$ $min^{-1}$.

The solid fat content (SFC) of the hydrogenated products was determined by pulse NMR method in accordance with ISO 8292 [26] using a spectrometer (NMR Minispec PC 20). The hydrogenated products were cooled to 0 °C for 60 min and thermostated at the 35 °C for 30 min.

## 3. Results and discussion

### 3.1. Characterization of the support and precursors

#### 3.1.1. X-ray diffraction (XRD)

The XRD pattern of the diatomite support (Fig. 1) shows reflections characteristic for amorphous silica (silica halo peak centered at $2\theta = 21°$) and well-crystallized quartz phase ($2\theta = 26.5°$; JCPDS 46-1045). The diffractograms of the non-reduced precursors are considerably different from the spectrum of the support (Fig. 1a). Two kinds of reflections are registered: nickel silicate hydroxide phase at $2\theta = 10.2$, 21.1, 24.2, 34.5 and 60.1° ($Ni_3Si_2O_5(OH)_4$, JCPDS 22-0754) and antigorite phase at $2\theta = 25$, 35.7, 36.3, 41.5 and 54.7° ($Mg_3Si_2O_5(OH)_4$, JCPDS 21-0963). The observed phenomenon proves that during the synthesis an interaction occurs between Ni salt and the support resulting in formation of nickel hydrosilicate layers, which covered the external surface of the silica particles. The nickel hydrosilicates are always formed during the precipitation of nickel nitrate and alkali silicate solutions at temperature below 100 °C. Their XRD patterns are not clearly defined due to its turbostratic structure [16,27–29]. Beside main lines of the nickel hydrosilicate some additional lines located at $2\theta = 32.4$, 33.7, 39.3 and 51.4°, characteristics of $Ag_2CO_3$ phase (JCPDS 26-0339) are also present in the diffractograms of the silver containing precursors (Fig. 1a).

In general, the observed broadening of the diffraction lines indicates that all precursors are poorly crystalline materials whose mean particle size determination is practically impossible.

It is well known that the metallic nickel is the active phase in the process of vegetable oils hydrogenation. XRD patterns of the reduced-passivated precursors are illustrated in Fig. 1b. The diffraction lines at $2\theta = 44.6$, 51.9, 76.9 and 93.3° can be ascribed to the metallic nickel phase (JCPDS 4-0850). The presence of Ni hydrosilicate phases indicates that the reduction of $Ni^{2+}$ species at 430 °C is not complete. Similar results have been reported in the literature for the incomplete reduction of nickel hydrosilicates at moderate temperatures [16,28,30].

Sharp diffraction lines located at $2\theta = 37.9$, 44.2, 64.2 and 76.9° are observed in the reduced silver containing precursors (Fig. 1b). These lines can be attributed to the metallic silver phase (JCPDS 4-0783). The reflections are significantly narrower and more intensive in the diffractogram of the precursor with higher silver content ($AgNi\text{-}0.1_{red}$). The XRD results reveal that the modification with silver provokes better crystallization of the corresponding silver phase in both non-reduced and reduced materials.

It is necessary to mention that the most intensive peak of the metallic nickel phase ($2\theta \sim 44.5°$) overlaps the second in intensity diffraction line of the metallic silver phase ($2\theta \sim 44.2°$). That is why the estimation of the metallic nickel crystallite size is done from the reflection situated at $2\theta \sim 51.9°$. The results show that the values of Ni° particles of all reduced precursors are located in the nanosize region, namely: 7.0 nm ($Ni\text{-}0_{red}$), 5.4 nm ($AgNi\text{-}0.025_{red}$) and 4.5 nm ($AgNi\text{-}0.1_{red}$). These data give us the reason to state that the dispersion of the active metallic nickel phase in the modified samples increases with the increase of the silver content.

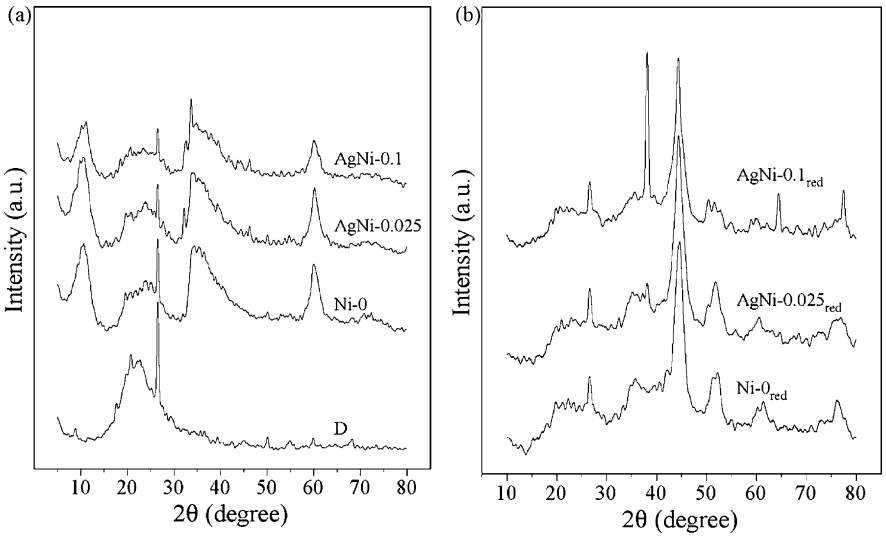


**Fig. 1.** XRD patterns of the support, non-reduced (a) and reduced (b) precursors.

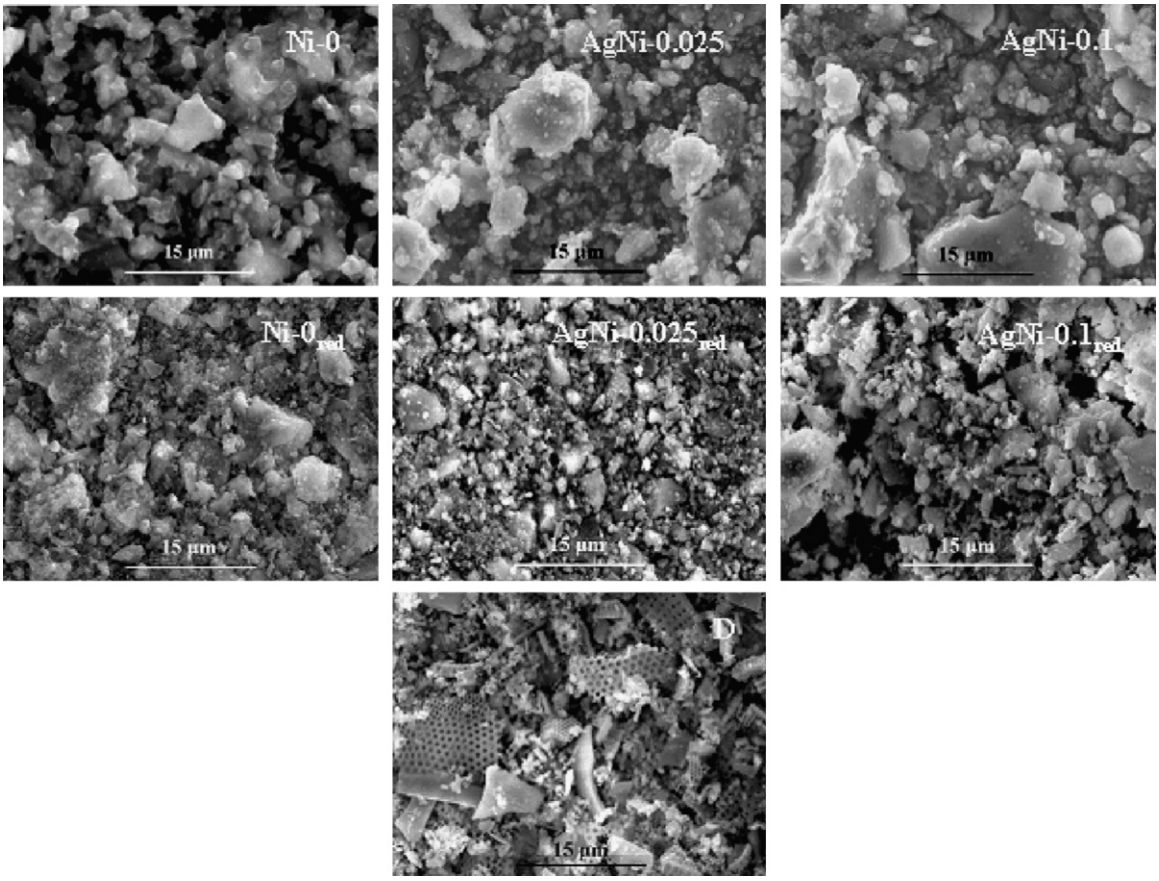


**Fig. 2.** SEM images of diatomite support (D), non-reduced and reduced precursors.

The increase of the silver content in the samples is responsible for the decrease of Ni° crystallites.

The size of the metallic silver crystallites is possible to be calculated only in the case of the AgNi-0.1$_{red}$ precursor from the most intensive peak at $2\theta \sim 38°$. It is obvious that silver crystallites are significantly larger (26 nm) than those of the metallic nickel ones.

It can be summarized that the modification of the Ni–Mg/$SiO_2$ precursor by Ag addition causes partial amorphisation of the structure of the non-reduced and reduced precursors. Moreover, it influences the degree of Ni° phase crystallisation and leads to the formation of relatively smaller Ni° particles.

### 3.1.2. Scanning electron microscopy (SEM)

SEM image of diatomite shows that the support surface is consisted of particles differing in kind, shape and size (Fig. 2). The non-reduced Ni–Mg and Ag–Ni–Mg precursors demonstrate well-pronounced and more homogeneous habit than the bare support. Fragments different in size and covered with many fine particles can be observed.

The reduction process causes changes in the sample morphology. Smaller size fragments are visible in the images of all reduced samples (Fig. 2).

### 3.1.3. Mercury intrusion porosimetry

Table 1 presents Hg-porosimetry data obtained for the diatomite support, non-reduced and reduced precursors. The measurements confirm well-known macropore character of the diatomite. The support has high total cumulative pore volume ($V_{tot\ cum}$) and total porosity ($P$). The macropore volume ($V_{macro}$) prevails and almost approaches to the $V_{tot\ cum}$. All non-reduced precursors show

**Table 1**
Summary of Hg-porosimetry data for the support, non-reduced and reduced precursors.

| Sample code | $S$ ($m^2\ g^{-1}$) | $V_{tot\ cum}$ ($cm^3\ g^{-1}$)[a] | $V_{macro}$ ($cm^3\ g^{-1}$) | $P$ (%) | PD (nm)[b] |
|---|---|---|---|---|---|
| D | 11.7 | 1.447 | 1.413 | 66.6 | 495 |
| Non-reduced precursors | | | | | |
| Ni-0 | 13.5 | 0.067 | 0.014 | 13.3 | 20 |
| AgNi-0.025 | 12.1 | 0.092 | 0.021 | 16.4 | 30 |
| AgNi-0.1 | 9.6 | 0.112 | 0.084 | 20.5 | 47 |
| Reduced precursors | | | | | |
| Ni-0$_{red}$ | 6.7 | 0.129 | 0.110 | 24.6 | 77 |
| AgNi-0.025$_{red}$ | 6.8 | 0.135 | 0.115 | 25.5 | 79 |
| AgNi-0.1$_{red}$ | 6.7 | 0.144 | 0.127 | 29.0 | 86 |

[a] Total cumulative pore volume over measurement range: 7.5–15000 nm.
[b] Average pore diameter PD = 4 $V_{tot\ cum}/S$.

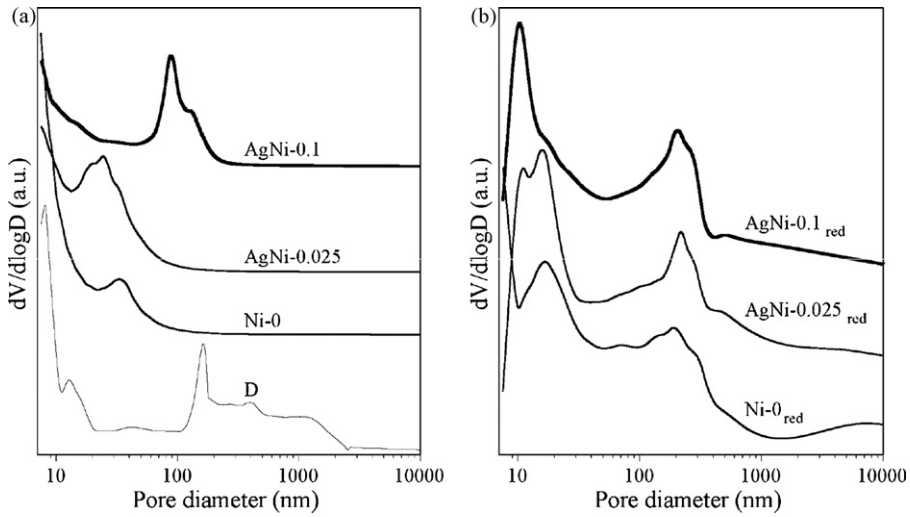


**Fig. 3.** PSD of the support, non-reduced (a) and reduced (b) precursors.

different porous structure than the support as a result of the components precipitation-deposition. A great diminution of $V_{tot\ cum}$ and $P$ of the support is observed. The silver addition to Ni-0 sample has a reverse effect resulting in the increase of $V_{tot\ cum}$, $V_{macro}$, PD (average pore diameter) and $P$ of the modified samples. The highest value of $V_{tot\ cum}$ (total intrusion pore volume) and the most developed macropore system are registered for the AgNi-0.1 precursor.

The reduction procedure further enhances macroporous characteristics of the reduced samples due to the formation of pores as a consequence of the $H_2O$ and $CO_2$ venting. It should be emphasized that the silver trend to promote expansion of macropores and increase the total porosity is preserved after the reduction procedure. A significant augmentation in the average pore diameter of the reduced precursors is observed (Table 1).

Pore size distribution curves over the entire pore diameters range (7.5–15000 nm) of the support and the precursors are shown in Fig. 3. The PSD curve of the support (Fig. 3a) indicates a polydisperse distribution in the macropores region. The formation of Ni-hydrosilicates onto the silica surface provokes changes in the PSD towards monodisperse porous structure. A shift towards the mesopores region is obvious for Ni-0 sample (Fig. 3a). The presence of silver additionally affects the texture of Ni-0 precursor depending on the modifier loadings. A small amount of silver (AgNi-0.025) slightly increases the value of PD, while higher quantity of silver (AgNi-0.1) redistributes the pores to the macroporous region.

PSD curves of the reduced precursors (Fig. 3b) show a bi-disperse pore system revealing some new effects such as equalization of the prevailing pore diameters range (Table 1) associated with a significant growth of PD comparing to its value in the non-reduced samples.

It can be concluded that the textural characteristics of the diatomite support are strongly influenced by the nickel and silver presence. Moreover, it is very important that the modification of nickel catalysts with silver provokes the development of meso- and macroporous structure, which can improve the access of triacylglycerol molecules to the internal surface. Large pores may facilitate the transfer of liquid oil from the exterior of the catalyst to the interior where smaller pores may be fed with it. It seems that silver-modified nickel catalysts have suitable porous structure for the use in the processes of edible oil hydrogenation where the diffusion control is likely to hinder the transfer to the interior. One would expect an improvement in the catalyst performance of the silver containing samples.

### 3.1.4. $H_2$-chemisorption

The metallic surface area of the reduced precursors is determined by $H_2$-chemisorption at 25 °C. It is well known that metallic silver does not chemisorb hydrogen at room temperature [31] and the experiment therefore was performed for the estimation of the metallic nickel surface area. The following order is established: Ni-$0_{red}$ > AgNi-$0.025_{red}$ > AgNi-$0.1_{red}$ (Table 2). It can be seen that the non-modified sample chemisorbs the largest amount of hydrogen corresponding to the highest nickel surface area ($S_{Ni}$) and specific nickel surface area ($S_{spNi}$). However, $H_2$ uptake of the modified samples decreases with increasing loading of silver. As a result, the values of $S_{Ni}$ and $S_{spNi}$ diminish. Apparently, the modification of Ni–Mg sample with silver decreases the hydrogen adsorption capacity of the metallic nickel depending on the Ag/Ni ratio.

A possible interpretation of the lower $H_2$ uptake of the modified samples may be found in our former study on the basis of *in situ* $H_2$-XRD experiments performed on the same samples [32]. It was found that $Ag^+$ ions in the modified precursors are reduced to the metallic silver prior to reaching the final reduction temperature of 430 °C. Evidently, $Ag^+$ ions are more easily reduced than $Ni^{2+}$ ones due to the general property of silver to interact weakly with most of the oxide surfaces, especially with $SiO_2$, forming two- or three-dimensional clusters depending on the extent of the silver coverage [33]. Lower surface energy of silver [34] would facilitate its migration onto the $Ni^{2+}$ species. As the result, partial covering of $Ni^{2+}$ entities is taking place, thus preventing the contact with hydrogen.

The metallic nickel surface area has predominant importance for the catalytic hydrogenation activity [35,36]. Considering that the involved reaction takes place on the surface of the catalyst, larger Ni° surface area obtained for the non-modified sample presumes larger number of active sites, namely nickel surface atoms where the reaction occurs. Consequently higher hydrogenation activity may be expected.

**Table 2**
$H_2$-chemisorption experiments on the non-modified and modified precursors.

| Sample code | $H_2$-uptake | Nickel surface area | |
|---|---|---|---|
| | ($\mu$mol $g^{-1}_{sample}$) | $S_{Ni}$ ($m^2_{Ni}$ $g^{-1}_{sample}$) | $S_{spNi}$ ($m^2_{Ni}$ $g^{-1}_{Ni}$) |
| Ni-$0_{red}$ | 265 | 20.7 | 58.2 |
| AgNi-$0.025_{red}$ | 189 | 14.8 | 42.1 |
| AgNi-$0.1_{red}$ | 172 | 13.5 | 40.2 |

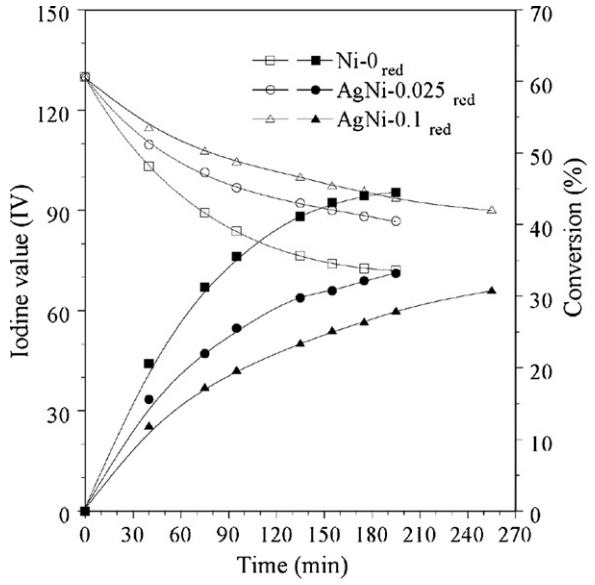


**Fig. 4.** IV and conversion *vs* time: empty symbols – IV and filled symbols – conversion.

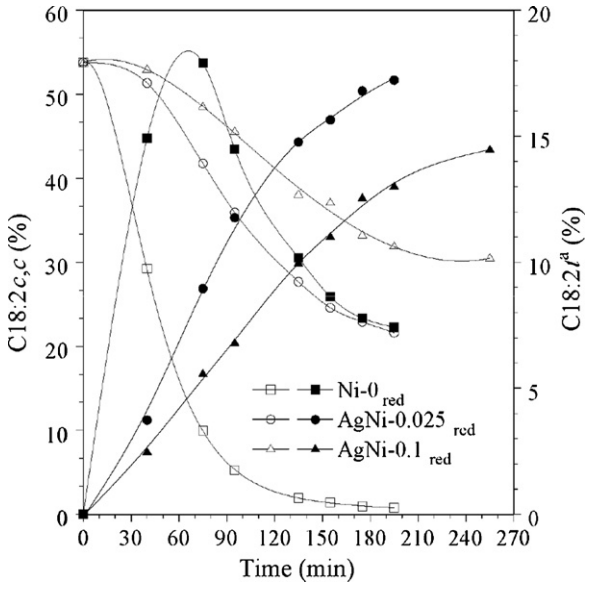


**Fig. 5.** C18:2 fatty acids profiles *vs* time: empty symbols – C18:2*c*,*c* and filled symbols – C18:2*t*[a]. ([a]Sum of *cis–trans* (*c*,*t*), *trans–cis* (*t*,*c*), *trans–trans* (*t*,*t*).)

### 3.2. Activity and selectivity

The soybean oil hydrogenation activity of the studied catalysts is represented as the change of the iodine value of the starting oil with the reaction time (Fig. 4).

It may be observed that IV decreases at the end of the reaction from 130 (crude oil) to 72, 87, and 90 using the catalysts Ni-$0_{red}$, AgNi-$0.025_{red}$ and AgNi-$0.1_{red}$, respectively. In addition, if the criterion for the catalyst activity is the reaction time necessary for the IV of about 90 to be reached, corresponding to the partially hydrogenated oil, the following results are obtained: 75 min (Ni-$0_{red}$), 155 min (AgNi-$0.025_{red}$) and 255 min (AgNi-$0.1_{red}$). The higher IV and the longer reaction time of the silver modified catalysts than the non-modified one indicate their lower soybean oil hydrogenation activity.

The catalytic activity data are in accordance with the results from $H_2$-chemisorption measurements, both related to the lower metallic nickel surface area of the silver modified precursors. As it is well known, the hydrogenation of vegetable oils is a structure insensitive reaction [35,37], and the catalytic activity of the employed catalysts depends mostly on the accessible metal active sites on the catalyst surface.

The differences in the activity of the studied catalysts reflect on the different fatty acid profiles obtained during the soybean oil hydrogenation (Figs. 5–8) and different composition of the fatty acids (Table 3). Concomitant with the hydrogenation, both reactions of geometric *cis–trans* and positional isomerization take place.

**Table 3**
Fatty acid composition in the partial hydrogenated soybean oil[a].

| Fatty acids (wt%) | Catalyst code | | |
|---|---|---|---|
| | Ni-$0_{red}$ | AgNi-$0.025_{red}$ | AgNi-$0.1_{red}$ |
| C18:0 | 7.2 | 5.9 | 5.6 |
| C18:1*t* | 48.6 | 15.7 | 10.0 |
| C18:1*c* | 14.8 | 21.4 | 21.5 |
| C18:2*t*[b] | 7.4 | 17.2 | 13.0 |
| C18:2*c*,*c* | 0.8 | 21.6 | 31.9 |
| Rest | 21.2 | 18.2 | 18.0 |

[a] Experimental conditions: $T = 160\,^{\circ}C$, $P = 0.16$ MPa, reaction time = 195 min.
[b] Sum of *cis–trans* (*c*,*t*), *trans–cis* (*t*,*c*), and *trans–trans* (*t*,*t*).

Since the present work is focused on the control of the *trans* fatty acid isomers and stearic acid content, the isomerization reactions are presented, without taking into account the position of double bond in the fatty acid chain, but distinguishing *cis* and *trans* isomers [38]. In all the cases, there is a decrease in linoleic acid, C18:2*c*,*c*, (Fig. 5) and an increase of stearic acid, C18:0 (Fig. 7) concentration, related to the hydrogenation of the double bonds. The linolenic acid, C18:3*c*,*c*,*c* (not shown) is completely hydrogenated within the first 40 min due to the high activity of the non-modified catalyst and much higher preference of the silver modified catalysts for linolenic over linoleic acid [11].

The double bonds in non-hydrogenated oil fatty acids are originally in *cis* conformation. Since *trans* isomers are thermodynamically more stable, they are invariably produced during the hydrogenation. In the case of non-modified catalyst, the *trans* isomers of linoleate rapidly increased, initially reaching maximum

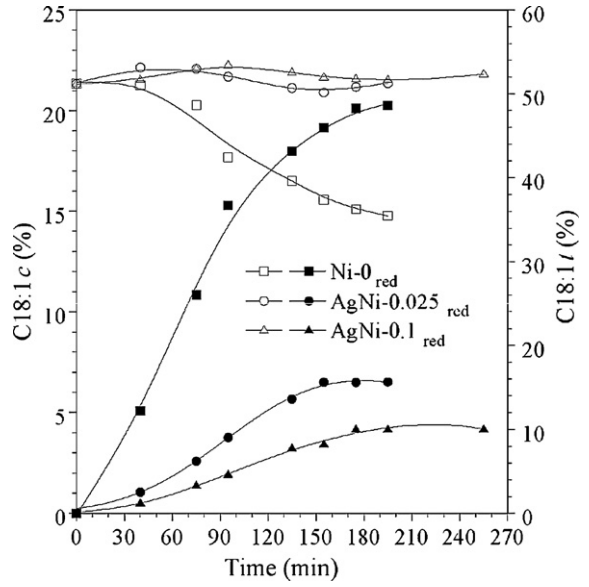


**Fig. 6.** C18:1 fatty acids profiles *vs* time: empty symbols – C18:1*c* and filled symbols – C18:1*t*.

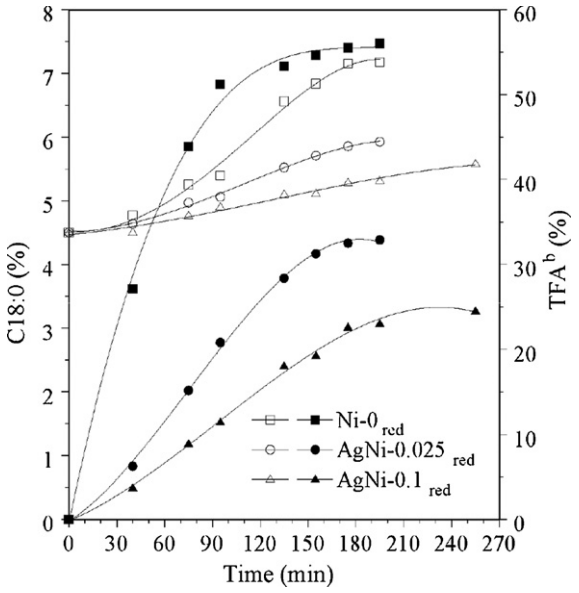


**Fig. 7.** C18:0 and TFA[b] profiles *vs* time: empty symbols – C18:0 and filled symbols – TFA (TFA[b] = C18:*xt* (*x* = 1 and 2)).

value of about 18% after 75 min, then leveled off as hydrogenation proceeded (Fig. 5). The linoleate *trans* isomers formation using the modified catalysts increased continuously with the reaction time. Meanwhile, elaidate, the *trans* isomer of oleate also increased continuously with the reaction time (Fig. 6). The hydrogenation of unsaturates resulted in the formation of larger amount of elaidate (~48%) in the presence of the non-modified catalyst. For the modified catalysts, AgNi-0.025$_{red}$ and AgNi-0.1$_{red}$, the content of *trans* isomers at the end of the reaction was significantly lower ~16% (AgNi-0.025$_{red}$) and ~10% (AgNi-0.1$_{red}$).

The general trend of results obtained for the CFA/TFA ratio (CFA – unsaturated C18:*yc* fatty acid; TFA – the corresponding C18:*xt* fatty acid) over non-modified and modified catalysts are demonstrated in Fig. 8. In the partially hydrogenated oil CFA/TFA ratio is an indication of the *trans* selectivity of the hydrogenation reaction. More

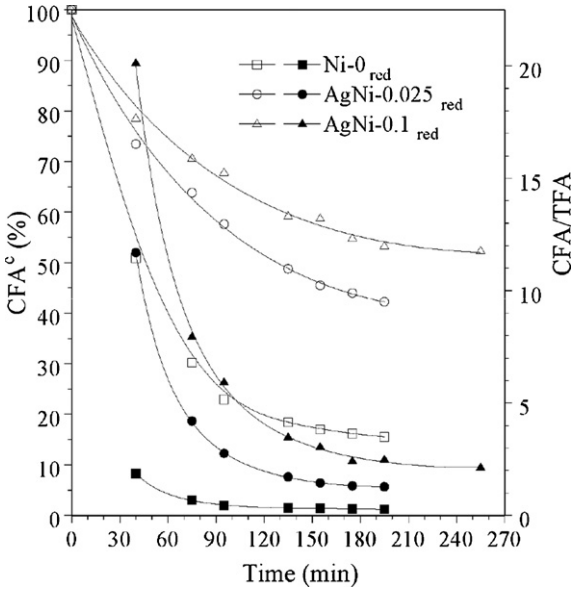


**Fig. 8.** CFA[c] and CFA/TFA profiles *vs* time: empty symbols – CFA and filled symbols – CFA/TFA (CFA[c] = C18:*yc* (*y* = 1 and 2)).

**Table 4**
Composition of C18:*z* fatty acid, selectivity and SFC in the partial hydrogenated soybean oil[a].

| C18:*z* fatty acid composition (wt%)[b] | Catalyst code | | |
|---|---|---|---|
| | Ni-0$_{red}$ | AgNi-0.025$_{red}$ | AgNi-0.1$_{red}$ |
| C18:0 | 7.2 | 5.9 | 5.6 |
| C18:1*t* | 36.7 | 15.6 | 10.0 |
| C18:1*c* | 17.7 | 20.9 | 21.8 |
| C18:2*t*,*t* | 3.2 | 2.1 | 1.9 |
| C18:2*c*,*t* | 5.4 | 6.5 | 6.4 |
| C18:2*t*,*c* | 5.9 | 7.0 | 6.3 |
| C18:2*c*,*c* | 5.3 | 24.6 | 30.5 |
| CFA/TFA | 0.4 | 1.5 | 2.1 |
| C18:0/TFA | 0.10 | 0.18 | 0.23 |
| $S_{Lo}$[c] | – | – | 0.4 |
| $S_i$[d] | 131.0 | 78.2 | 61.7 |
| $R_t$ (%)[e] | – | 38.9 | 52.2 |
| Conversion (%) | 30.1 | 30.8 | 30.6 |
| IV | 90.9 | 90.0 | 90.3 |
| SFC$_{35\,°C}$ | 3.08 | 1.04 | 0.72 |

[a] Experimental conditions: T = 160 °C, P = 0.16 MPa.
[b] *z* = 0, 1 and 2.
[c] Linoleic selectivity: $S_{Lo} = \Delta C_{C18:1c}/\Delta C_{C18:0}$ [11].
[d] Specific isomerization: $S_i = -100(\Delta C18{:}yt^f/\Delta(IV))$, *y* = 1 and 2 [11].
[e] *trans* reduction: $R_i = 100(1 - (\Delta C18{:}yt^f)_{cat2}/(\Delta C18{:}yt^f)_{cat1})$, $(\Delta C18{:}yt^f)_{cat1} > (\Delta C18{:}yt^f)_{cat2}$ ($^f$sum of *cis–trans* (*c*,*t*), *trans–cis* (*t*,*c*), and *trans–trans* (*t*,*t*)).

particularly, a higher ratio of CFA/TFA suggests a lower *cis–trans* isomerization of an adsorbed carbon–carbon double bond on the catalyst surface.

CFA/TFA ratio of the studied catalysts was high at the beginning of the hydrogenation but decreased with the reaction time. At any moment of the hydrogenation using the non-modified catalyst the oil contains C18:*yc* and C18:*xt* fatty acids with the lowest ratio of CFA/TFA. Higher ratio of unsaturated *cis* fatty acids to *trans* fatty acids over AgNi-0.1$_{red}$ catalyst can be attributed to the smaller formation of *trans* fatty acids, suggesting a more selective hydrogenation reaction.

In general, the overall hydrogenation selectivity decreased while the isomerization increased with conversion. Since hydrogenation and isomerization vary with conversion, the selectivity values were compared at the same conversion level.

Table 4 summarizes the fatty acids composition over Ni-0$_{red}$, AgNi-0.025$_{red}$ and AgNi-0.1$_{red}$ catalysts at the conversion of 30%. Fractions of hydrogenated soybean oil over the studied catalyst samples were compared at IV of about 90. This value corresponds to the IV of the final hydrogenated oil fraction when the reaction was performed over the catalyst with the lowest activity (sample AgNi-0.1$_{red}$). It can be observed that the non-modified catalyst generated more *trans* isomers than the silver modified ones. The addition of silver to nickel had significant effect on the *trans* isomerization under the studied conditions. For both Ag/Ni ratios, a considerable decrease of C18:1*t* *trans* isomers that are most detrimental was achieved, and it was higher on the catalysts with higher silver loading (Table 4). Therefore, it can be concluded that the modification with silver is beneficial in limiting the C18:1 *cis–trans* isomerization during the soybean oil hydrogenation on nickel. On the other hand, the introduction of silver did not have significant effect on the formation and distribution of C18:2*t* (sum of *cis–trans*, *trans–cis*, and *trans–trans*) isomers, indicating that the main cause of the difference in the specific isomerization selectivity ($S_i$) was the favored isomerization of C18:1*t* over Ni-0$_{red}$ catalyst. At the same time the formation of stearic acid is slightly decreased in the presence of silver, thus improving the linoleic selectivity ($S_{Lo}$) of the modified catalyst. It should be noted that this selectivity was negative for the hydrogenation with Ni-0$_{red}$ and AgNi-0.025$_{red}$ catalysts, because

oleic acid was hydrogenated to stearic one more rapidly than it was formed from linoleic acid. Concerning the $S_i$ of the reaction, the addition of silver provoked decrease of the total amount of *trans* isomers ($R_t$) in the range of 38–53% during the soybean oil hydrogenation with respect to the non-modified catalyst.

Partially hydrogenated oil contains unsaturated fatty acids as well as *trans* isomers. The latter are a principal objective in solid shortening and margarine products because of their ability to contribute, parallelly with the saturated acids, to higher melting and crystallization properties. Hydrogenated fats being complex mixtures do not have a sharp melting point but a rather wide melting range. A measure of the crystallized fat content at a series of temperature checkpoints represents the solid fat content as a function of the temperature. If the fat contains high-melting triglycerides, the value of SCF would be high at relatively high temperature. With regard to this, the quantity of SFC is generally related to the selectivity and is an indicative of the utility of the hydrogenated oil [39].

The values of SFC at 35 °C were obtained by partial hydrogenation of soybean oil up to IV of about 90 (Table 4). The non-modified Ni-$0_{red}$ catalyst produced greater amount of SF than the modified ones. The smallest SFC value was observed for the catalyst with higher silver loading, AgNi-$0.1_{red}$ that corresponds to the lowest content of stearic acid and total *trans* isomers.

The limited formation of stearic acid in the presence of silver-modified catalysts (Tables 3 and 4) may be explained on the basis of the textural properties of the reduced samples (Table 2). According to Balakos and Hernandez [36], the presence of pores with small diameters (unmodified Ni-$0_{red}$ catalyst) favors the hydrogenation process to stearic acid, because the saturated triacylglycerols posses the smallest molecule size, which facilitates their desorption ability.

On the contrary, the lower hydrogenation activity manifested by the modified catalysts in comparison to the non-modified one (Table 4) could neither be explained on the basis of their texture (development of macropores and increase of the total porosity) nor from XRD (higher dispersion of the active metallic nickel phase) and morphology (fine-grained materials) studies of the reduced precursors. In addition, the above mentioned textural data are not able to interpret the limiting of *cis–trans* isomerization over silver-containing catalysts, because the transport of triacylglycerol molecules easily takes place in larger pores, and as a consequence, the molecules would have more chance of isomerization prior to hydrogenation of the unsaturated bonds [40].

Evidently, the textural properties partially explain the effect of silver on the catalyst performance. Another probable explanation may be attributed to NiAg alloy formation. However, it is well known that silver and nickel do not form a solid solution at any composition under equilibrium conditions [41]. Metastable NiAg alloys have been observed in specific circumstance. These alloys give rise to phase separation and reformation of individual nickel and silver nano-particles with time on stream [42].

The lower hydrogen adsorption capacity, reduced hydrogenation activity and limited *cis–trans* isomerization demonstrated by the silver-modified samples may be interpreted on the basis of the Horiuti–Polanyi mechanism describing the hydrogenation and isomerization of light olefins [43].

According to this mechanism, both hydrogenation and isomerization proceed at the same active sites *via* the half-hydrogenated intermediates including different stepwise addition and elimination of hydrogen atoms. The number of the active metallic nickel sites on the surface of AgNi-$0.025_{red}$ and AgNi-$0.1_{red}$ catalysts diminishes, due to the migration of the metallic silver over $Ni^{2+}$ species. This feature provokes covering and blocking of $Ni^{2+}$ entities, hampering the hydrogen ability to reduce them to metallic nickel as evidenced by $H_2$-chemisorption. On the other hand, this phenomenon is beneficial in limiting the C18:1 *cis–trans* izomerization. In addition, it does not strongly influence the proportion of saturated C18:0 fatty acid. Moreover, taking into account the smaller quantity of solid components in the hydrogenated products it may be stated that the silver modified Ni-Mg/diatomite catalysts exhibit better selectivity.

## 4. Conclusions

The modification of the Mg–Ni/diatomite precursor by Ag addition causes partial amorphisation of the poorly crystallized antigorite-like Ni-hydrosilicates in the as-synthesized materials and the formation of smaller Ni° crystallites in the reduced precursors.

The increase of the silver loading provokes the development of macroporosity thus increasing total sample porosity. The reduction procedure further enhances macroporous characteristics of the reduced samples thus limiting the formation of the non-desirable stearic acid.

The migration of metallic silver onto $Ni^{2+}$ entities impedes their reduction to the metallic state thus leading to decrease of the number of metallic nickel sites on the surface as evidenced by $H_2$-chemisorption of the modified precursors.

The decreases of both $H_2$-adsorption capacity and hydrogenation activity of the modified precursors may be related to the metallic silver covering and blocking effects on the $Ni^{2+}$ species, thus hampering the access of hydrogen. Contrariwise, the silver presence is beneficial in limiting the C18:1 *cis–trans* isomerization. Horiuti–Polanyi mechanism based on the assumption that hydrogenation and isomerization proceed at the same active sites *via* the half-hydrogenated intermediates supplies the most plausible explanation of the effect of silver modification.

Adjustment of the catalyst composition by changing the content of silver modifier offers a possibility to control the total amount of the detrimental *trans* fatty acid isomers, stearic acid and solid fat content in the hydrogenated derivatives.

The catalyst with higher silver content seems to be a more promising catalyst for the selective edible oil hydrogenation.

## Acknowledgements

The authors (M.G., P.Tz., M.S., Ts.Ts. and R.K.) are grateful to the National Science Fund at the Ministry of Education and Science of Bulgaria for the partial financial support (Project X-1411).

The authors (M.St., J.K., P.B. and D.J.) greatly acknowledge the support of the Serbian Ministry of Science through the Project 166001B.

## References

[1] M. Fernández, G. Tonetto, G. Crapiste, D. Damiani, J. Food Eng. 82 (2007) 199–208.
[2] R. O'Brien, Fats and Oils: Formulating and Processing for Applications, 2nd ed., CRC Press LLC, 2004.
[3] J. Weldsink, M. Bouma, N. Schöön, A. Beenackers, Catal. Rev. Sci. Eng. 39 (1997) 253–318.
[4] K. Belkacemi, A. Boulmerka, J. Arul, S. Hamoudi, Topics Catal. 37 (2006) 113–120.
[5] M. Semma, J. Health Sci. 48 (2002) 7–13.
[6] G. Yusem, P. Pintauro, J. Am. Oil Chem. Soc. 69 (1992) 399–404.
[7] A. Santana, M. Larrayoz, E. Ramírez, J. Nistal, F. Recasens, J. Supercrit, Fluids 41 (2007) 391–403.
[8] D. Fritsch, G. Bengtson, Catal. Today 118 (2006) 121–127.
[9] M. Tike, V. Mahajani, Chem. Eng. J. 123 (2006) 31–41.
[10] T. Boger, M. Zieverink, M. Kreutzer, F. Kapteijn, J. Moulijn, W. Addiego, Ind. Eng. Chem. Res. 43 (2004) 2337–2344.
[11] J. Van Lefèbvre, J. Baltes, Fette Seifen Anstrichmittel 77 (2) (1975) 125–131.
[12] A. Wright, A. Wong, L. Diosady, Food Res. Int. 36 (2003) 1069–1072.

[13] B. Nohair, C. Especel, P. Marécot, C. Montassier, L. Hoang, J. Barbier, C. R. Chimie 7 (2004) 113–118.
[14] B. Nohair, C. Especel, G. Lafaye, P. Marécot, L. Hoang, J. Barbier, J. Mol. Catal. A: Chem. 229 (2005) 117–126.
[15] K. Belkacemi, N. Kemache, S. Hamoudi, J. Arul, Int. J. Chem. Reactor Eng., 5 (2007) Article A116.
[16] J. Coenen, Ind. Eng. Chem. Fundam. 25 (1986) 43–52.
[17] S. Echeverria, V. Andres, Appl. Catal. 66 (1990) 73–90.
[18] D. Jovanović, R. Radović, Lj. Mareš, M. Stanković, B. Marković, Catal. Today 43 (1998) 21–28.
[19] M. Gabrovska, J. Krstić, R. Edreva-Kardjieva, M. Stanković, D. Jovanović, Appl. Catal. A: General 299 (2006) 73–83.
[20] M. Gabrovska, D. Nikolova, M. Stanković, R. Edreva-Kardjieva, D. Jovanović, Physical chemistry 2006, in: Proc. 8th Int. Conf. Fundam. Appl. Aspects Phys. Chem, 26–29 September, Belgrade, Serbia, 2006, pp. 165–167.
[21] M. Stanković, J. Krstić, M. Gabrovska, P. Banković, D. Jovanović, XIII Workshop über die Charakterisierung von feinteiligen und porösen Festkörpern, 14–15 November, Bad Soden, Germany (2006).
[22] www.unipress.waw.pl./fityk
[23] Animal and vegetable fats and oils: Determination of iodine value. Standard method: ISO 3961 (1996).
[24] International Union of Pure and Applied Chemists, Standard Methods for the Analysis of Oils and Derivatives, Pergamon, Oxford, Part I (Section 1 and 22), 6th ed. (1979).
[25] M. Naglič, A. Šmidovnik, J. Chromatogr., A 767 (1997) 335–339.
[26] Animal and vegetable fats and oil – determination of solid fat content – pulsed nuclear magnetic resonance method. Standard Method ISO 8292 (1991)].
[27] J. van Eijk van Voorthuijsen, P. Franzen, Rec. Trav. Chim. 70 (1951) 793–812.
[28] K. Ghuge, A. Bhat, G. Babu, Appl. Catal. A: Gen. 103 (1993) 183–204.
[29] P. Burattin, M. Che, C. Louis, J. Phys. Chem. B 101 (1997) 7060–7074.
[30] M. Montes, Ch. Penneman de Bosscheyde, B. Hodnett, F. Delannay, P. Grange, B. Delmon, Appl. Catal. 12 (1984) 309–330.
[31] J. Anderson, Structure of Metallic Catalysts, Academic Press, New York, 1975.
[32] M. Gabrovska, P. Tzvetkov, D. Mucha, M. Stanković, J. Krstić, R. Edreva-Kardjieva, D. Jovanović, in: E. Balabanova, I. Dragieva (Eds.), Nanoscience & Nanotechnology, 7, Sofia, Bulgaria, Heron Press, 2007, pp. 274–277.
[33] Y.D. Kim, T. Wei, S. Wendt, D.W. Goodman, Langmuir 19 (2003) 7929–7932.
[34] E. Cottancin, M. Gaudry, M. Pellarin, J. Lermé, L. Arnaud, J. Huntzinger, J. Vialle, M. Treilleux, P. Mélinon, J.-L. Rousset, M. Broyer, Eur. Phys. J. D 24 (2003) 111–114.
[35] J. Coenen, B. Linsen, Structure and activity of silica-supported nickel catalysts, in: B. Linsen (Ed.), in: J. Fortuin, C. Okkerse, J. Steggerda (Co-eds.). Physical and Chemical Aspects of Adsorbents and Catalysts, Academic Press, New York, 1970.
[36] M. Balakos, E. Hernandez, Catal. Today 35 (1997) 415–425.
[37] J. Coenen, in: B. Delmon, P. Grange, P.A. Jacobs, G. Poncelet (Eds.), Preparation of Catalysts. II., Elsevier, Amsterdam, 1979.
[38] D. Jovanović, Ž. Čupić, M. Stanković, Lj. Rožić, B. Marković, J. Mol. Catal. A: Chem. 159 (2000) 353–357.
[39] S. Koritala, J. Am. Oil Chem. Soc. 62 (1985) 517–520.
[40] B. Linsen, PhD Thesis, Uitgeverij Waltman, Delft, Netherlands, 1964.
[41] Binary Alloy Phase Diagrams, 2nd ed., In: T.B. Massalski, H. Okamoto, P. Subramanian, L. Kacprzak (eds.) (ASM International, Metals Park, OH, 1990).
[42] A. Kumar, Ch. Damle, M. Sastry, Appl. Phys. Lett. 79 (20) (2001) 3314–3316.
[43] I. Horiuti, M. Polanyi, Trans. Faraday Soc. 30 (1934) 1164–1172.